analytical chemistry

pubs.acs.org/ac Article

# Multifaceted Bioanalytical Methods for the Comprehensive Pharmacokinetic and Catabolic Assessment of MEDI3726, an Anti-Prostate-Specific Membrane Antigen Pyrrolobenzodiazepine Antibody–Drug Conjugate

Yue Huang, Christopher J. Del Nagro, Kemal Balic, William R. Mylott Jr., Omnia A. Ismaiel, Eric Ma, Morse Faria, Aaron M. Wheeler, Moucun Yuan, Michael P. Waldron, Marlking G. Peay, Diego F. Cortes, Lorin Roskos, Meina Liang, and Anton I. Rosenbaum*

Cite This: *Anal. Chem.* 2020, 92, 11135–11144

Read Online

ACCESS | Metrics & More | Article Recommendations | Supporting Information

**ABSTRACT:** Complex biotherapeutic modalities, such as antibody-drug conjugates (ADC), present significant challenges for the comprehensive bioanalytical characterization of their pharmacokinetics (PK) and catabolism in both preclinical and clinical settings. Thus, the bioanalytical strategy for ADCs must be designed to address the specific structural elements of the protein scaffold, linker, and warhead. A typical bioanalytical strategy for ADCs involves quantification of the Total ADC, Total IgG, and Free Warhead concentrations. Herein, we present bioanalytical characterization of the PK and catabolism of a novel ADC. MEDI3726 targets prostate-specific membrane antigen (PMSA) and is comprised of a humanized IgG1 antibody site-specifically conjugated to tesirine (SG3249). The MEDI3726 protein scaffold lacks interchain disulfide bonds and has an average drug to antibody ratio (DAR) of 2. Based on the structural characteristics of MEDI3726, an array of 4 bioanalytical assays detecting 6 different surrogate analyte classes representing at least 14 unique species was developed, validated, and employed in support of a first-in-human clinical trial (NCT02991911). MEDI3726 requires the combination of heavy-light chain structure and conjugated warhead to selectively deliver the warhead to the target cells. Therefore, both heavy-light chain dissociation and the deconjugation of the warhead will affect the activity of MEDI3726. The concentration–time profiles of subjects dosed with MEDI3726 revealed catabolism of the protein scaffold manifested by the more rapid clearance of the Active ADC, while exhibiting minimal deconjugation of the pyrrolobenzodiazepine (PBD) warhead (SG3199).



In 2019, prostate cancer was estimated to be the most common cancer among men in the United States and second worldwide.[1] It was also the second leading cause of death from cancer for men in the U.S.[1] Although most prostate cancer patients can be initially treated with androgen-deprivation therapy,[2] some patients develop resistance to the standard of care therapy over time and progress to castration-resistant prostate cancer (CRPC), which can then lead to metastatic CRPC (mCRPC).[3] Currently, mCRPC remains incurable.[4] Therefore, novel treatment development is necessary for mCRPC patients.

Early in the 1990s, prostate-specific membrane antigen (PSMA) was identified as one of the biomarkers that can identify patients with prostate cancer within the healthy population.[5−7] PSMA was found to be highly expressed in prostate cancers but very limited in normal tissues.[8−10] Highly specific antibodies were developed to recognize PSMA.[11] Soon thereafter, PSMA was validated as a diagnostic biomarker[12] as well as a potential target for therapeutic intervention.[13,14] PSMA-targeting antibodies were used as immunohistochemical markers for prostatic epithelial cells.[15] Diagnostic kits with radiolabeled anti-PSMA antibody for the identification of prostate cancer metastases were approved by the U.S. Food and Drug Administration (FDA).[12,16] As a membrane-bound antigen, the internalization properties of PSMA were also interrogated by anti-PSMA antibodies specifically targeting the extracellular domain.[17] The abundant expression, highly localized distribution, as well as the internalization properties

**Received:** March 18, 2020
**Accepted:** May 27, 2020
**Published:** May 27, 2020







https://dx.doi.org/10.1021/acs.analchem.0c01187
*Anal. Chem.* 2020, 92, 11135−11144

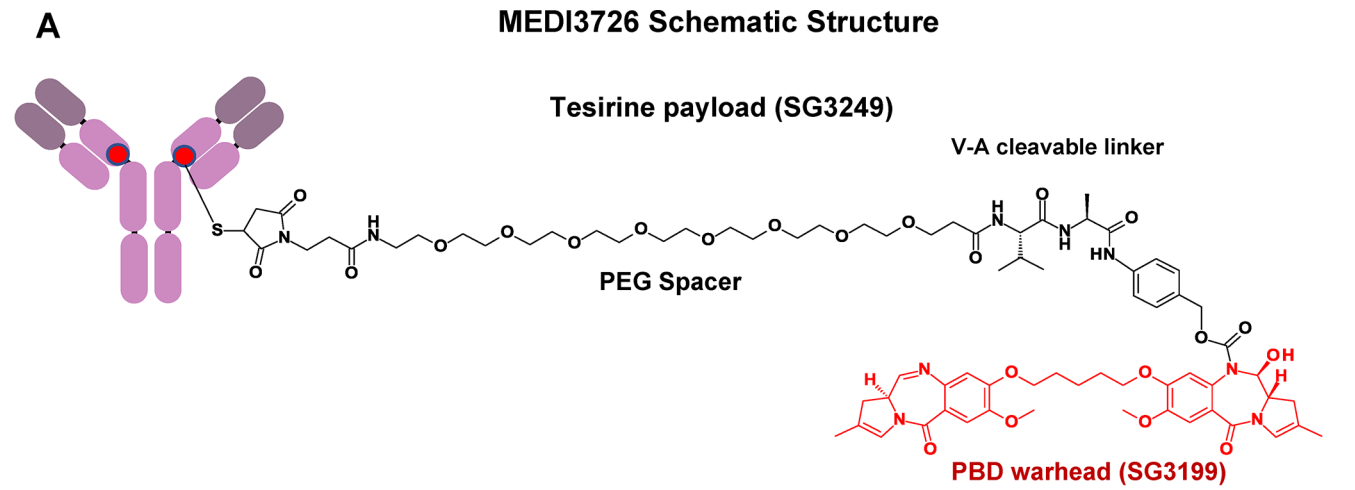


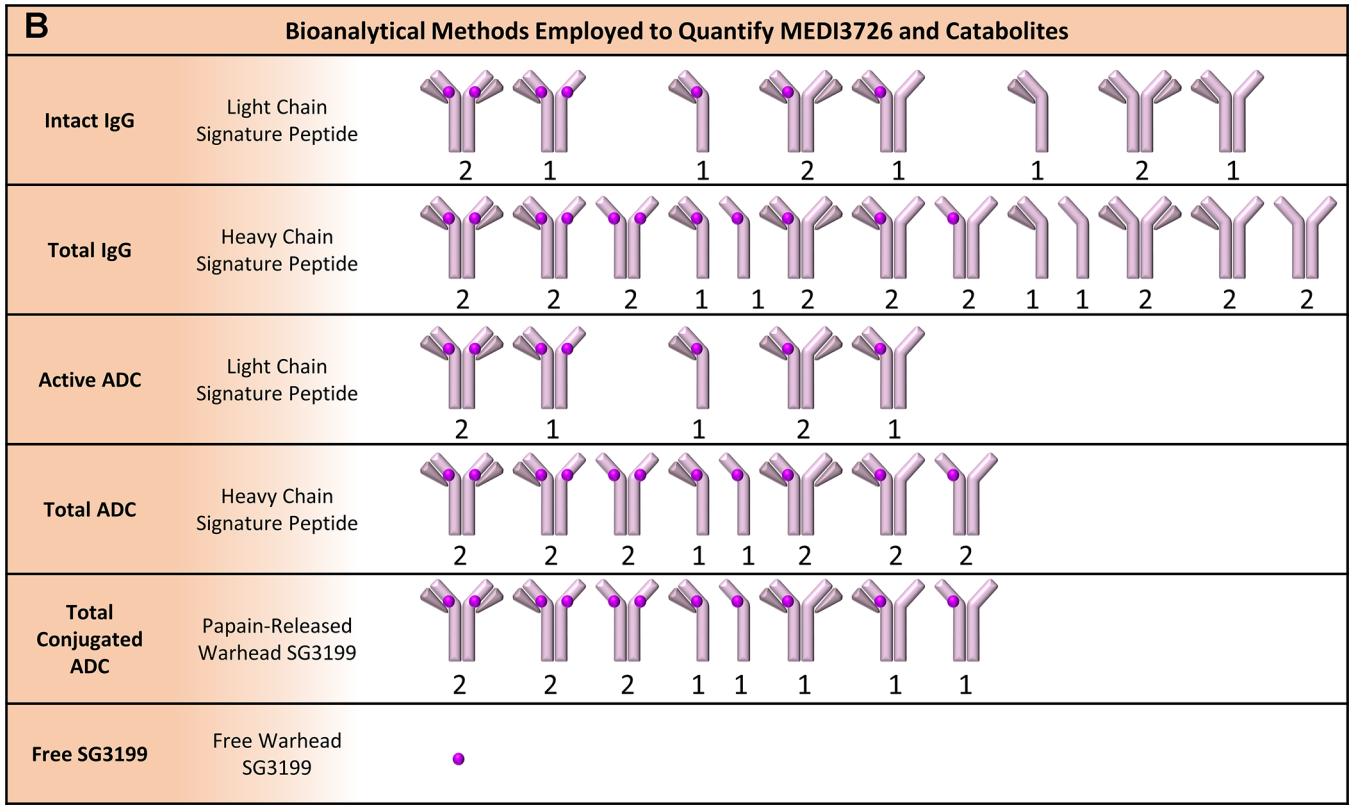


**Figure 1.** MEDI3726 schematic structure adapted from previous publication.[36] (A) Assay nomenclature and corresponding MEDI3726 catabolite species. The number below each species represents the molar stoichiometry of the surrogate analytes that would be measured in each specific assay format for each catabolite (B).

of PSMA provided the rationale for the development of the PSMA-targeting antibody−drug conjugate (ADC) therapy for mCRPC.[18−22]

ADCs have been designed to deliver cytotoxic small molecule drugs (warheads) to tumors or cancer cells by targeting tumor-specific antigens.[23] The ideal ADC target would be highly localized to tumors with suitable internalization properties.[24] Due to the targeted nature of the delivery of the toxin to tumors, ADCs can utilize highly cytotoxic warheads. Several ADCs have been approved over the years, including inotuzumab ozogamicin and gemtuzumab ozogamicin,[25] brentuximab vedotin and enfortumab vedotin,[26,27] as well as trastuzumab emtansine[28] and polatuzumab vedotin.[29] Recently, trastuzumab deruxtecan (DS-8201a) from Daiichi Sankyo has shown promising results from clinical trials against HER2-expressing, advanced solid tumors[30,31] and was approved in 2019 by the FDA for treatment of breast cancer.[32] Sacituzumab govitecan-hziy (IMMU-132), an anti-Trop-2/SN-38 ADC,[33] was approved by FDA for the treatment of metastatic triple-negative breast cancer in 2020. The structural design of an ADC encompasses the antibody, the warhead, linker chemistry, and conjugation site. Among the various classes of warheads that have been under clinical evaluation, DNA-intercalating pyrrolobenzodiazepine (PBD) dimer is one of the most potent classes of cytotoxic warheads.[34−37] Lysine or cysteine residues are usually employed as payload conjugation sites. Although the earlier technologies utilized mainly site-nonspecific conjugation, site-specific conjugation


https://dx.doi.org/10.1021/acs.analchem.0c01187
Anal. Chem. 2020, 92, 11135−11144

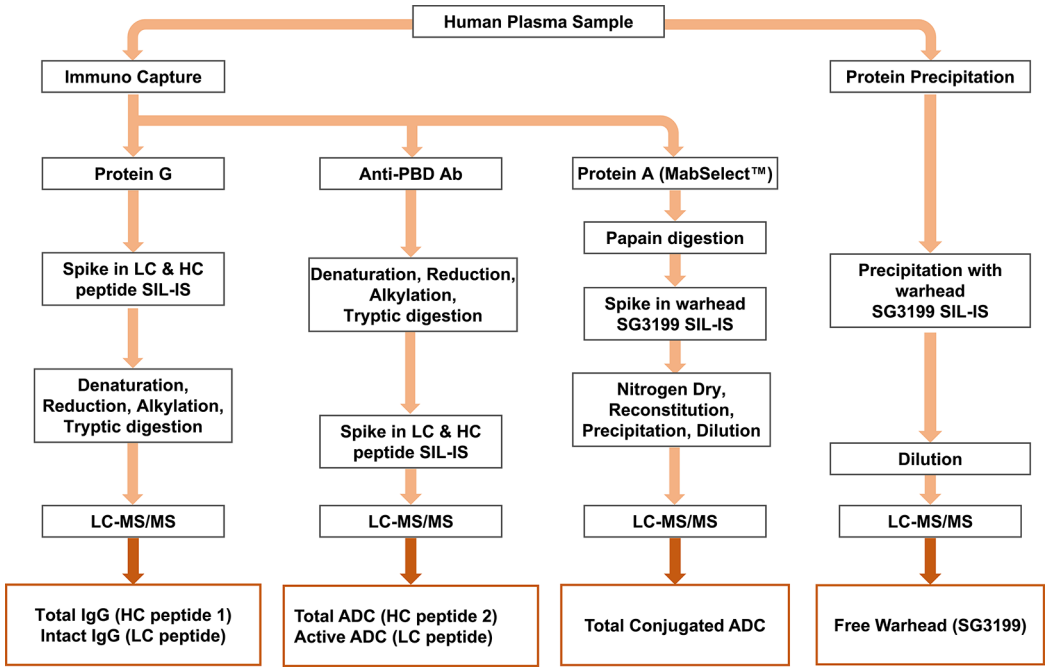


**Figure 2.** Flowchart of the bioanalytical methods for MEDI3726.

can reduce the heterogeneity of the ADC, which should lead to narrower DAR distribution and better controlled physicochemical properties of the ADC.[38]

MEDI3726 (also known as ADCT-401) consists of a PSMA-targeting antibody (also known as a humanized engineered J591) conjugated in a site-specific manner via maleimide to heavy chain C220 with tesirine (SG3249)[39,40] at a drug to antibody ratio (DAR) of approximately 2.[36] To ensure the correct conjugation site of the warhead, the following mutations were introduced: C214S in the light chain and C226V and C229V in the heavy chain. The structure of MEDI3726 was described previously[36] and is depicted in Figure 1A.

The typical bioanalytical strategy for ADCs involves quantification of the concentrations of the ADC, Total IgG, and Free Warhead.[38] However, since MEDI3726 interchain disulfide bonds were modified, this presented significant bioanalytical challenges with respect to comprehensive PK assessment of this ADC and its major catabolites (Figure 1B). Herein, we present the bioanalytical strategy and methods developed to characterize the PK of MEDI3726 and its potential catabolites from human plasma. The array of assays enabled the quantification of the concentrations of various species resulting from MEDI3726 catabolism (Figure 1B). In order to establish relatively simple and consistent nomenclature, the bioanalytical methods developed were denoted as (1) Active and Total ADCs, (2) Intact and Total Antibody, (3) Total Conjugated Warhead, as well as (4) Free Warhead. The detailed PK information obtained from all the assays enabled comprehensive multifaceted assessment of potential catabolites and their impact on the efficacy and safety of MEDI3726.

## MATERIALS AND METHODS

To differentiate between the various species of MEDI3726 and the associated catabolites, combinations of capture reagents and detection peptide/warhead were carefully selected. The diagram describing the detailed bioanalytical methods employed is presented in Figure 2.

**Reference and Internal Standards.** MEDI3726 and SG3199 reference standards were provided by MedImmune LLC (part of AstraZeneca), Gaithersburg, MD. Stable isotope-labeled internal standard (SIL-IS) peptides TSGY, ASQD, and GLEW were supplied by Elim Biopharmaceuticals, Hayward, CA. The warhead SIL-IS SG3199-d10 was supplied by Spirogen Ltd. (part of AstraZeneca), London, U.K.

**Capture Reagents.** Anti-PBD antibody was provided by MedImmune LLC (part of AstraZeneca), Gaithersburg, MD. Protein G magnetic beads were purchased from Millipore (Burlington, MA). The Streptavidin Dynabeads were purchased from Thermo Fisher Scientific (Waltham, MA). MabSelect beads were purchased from GE Healthcare (Chicago, IL). Information about the generic reagents is provided in the Supporting Information.

**Instruments.** For all four assays, the autosampler used was the LC PAL with DLW from CTC Analytics AG (Zwingen, Switzerland) and the LC system consisted of Agilent 1260 SL and 1100 series pumps. Mass spectrometry detection for the Total IgG and Intact IgG assays was performed with a SCIEX (Framingham, MA) 6500+ triple quadrupole mass spectrometer. All other assays employed a SCIEX 6500 triple quadrupole mass spectrometer for detection.

**Data Analysis.** Peak area integration and calculations of sample concentrations were performed with SCIEX (Framingham, MA) Analyst software, version 1.6.2. Representative chromatograms for each of the assays can be found in the Supporting Information, Figures S1−S6.

Noncompartmental analysis after the first dose of Cycle 1 was performed on the individual PK data using Phoenix WinNonlin (version 7.0, Certara, Princeton, NJ). The area under the plasma concentration−time curve was calculated using the linear/log trapezoidal rule. The area under the plasma concentration−time curve from time zero to infinity ($AUC_{0\text{-inf}}$) was calculated as the sum of $AUC_{0\text{-last}}$ and $C_{last}/\lambda_z$,


https://dx.doi.org/10.1021/acs.analchem.0c01187
Anal. Chem. 2020, 92, 11135−11144

**Table 1. Analyte and Internal Standard for the Four Assays and Six Surrogate Analytes**

| assay no. | assay name | quantitative range (ng/mL) | interassay precision[b] | interassay accuracy[b] | capturing reagent | analyte monitored | internal standard[a] | Q1/Q3 |
|---|---|---|---|---|---|---|---|---|
| 1 | Total IgG | 50−5000 | 5.28−12.1% | 1.37−11.9% | Protein G | GLEWIGNINPNNGGTTYNQK | GLEWIGNINPNNGGTTYNQK* | 1095.70/1193.70 (GLEW) |
| | | | | | | | | 1099.70/1201.70 (GLEW-IS) |
| | Intact IgG | 50−5000 | 6.72−13.0% | 0−8.49% | Protein G | ASQDVGTAVDWYQQKPGPSPK | ASQDVGTAVDWYQQK*PGPSPK* | 753.82/880.00 (ASQD) |
| | | | | | | | | 759.20/888.10 (ASQD-IS) |
| 2 | Total ADC | 10−2000 | 9.63−17.3% | −1.02−10.2% | Anti-PBD Ab | TSGYTFTEYTIHWVK | TSGYTFTEYTIHWV*K* | 917.05/1176.55 (TSGY) |
| | | | | | | | | 924.05/1190.55 (TSGY-IS) |
| | Active ADC | 10−2000 | 8.35−16.1% | −5.74−5.61% | Anti-PBD Ab | ASQDVGTAVDWYQQKPGPSPK | ASQDVGTAVDWYQQK*PGPSPK* | 753.82/880.00 (ASQD) |
| | | | | | | | | 759.20/888.10 (ASQD-IS) |
| 3 | Total Conjugated ADC | 0.0702−14.0[c] | 2.73−7.59% | 0.936−4.50% | Protein A | SG3199 | SG3199-d10 | 585.30/504.30 (SG3199) |
| | | | | | | | | 595.30/514.30 (SG3199-d10) |
| 4 | Free Warhead | 0.02−10.0 | 3.28−8.04% | −4.51 to −0.686% | NA | SG3199 | SG3199-d10 | 585.30/504.30 (SG3199) |
| | | | | | | | | 595.30/514.30 (SG3199-d10) |

[a]K* is $^{13}C_6$, $^{15}N_2$-Lysine, V* is $^{13}C_5$, $^{15}N$-Valine. [b]Interassay accuracy and precision data acquired during assay validation. [c]Total Conjugated ADC assay quantitative range equivalent to 10−2000 ng/mL of ADC.



https://dx.doi.org/10.1021/acs.analchem.0c01187
Anal. Chem. 2020, 92, 11135−11144

where $C_{last}$ is the last measurable concentration and $\lambda_z$ is the elimination rate constant. $AUC_{0\text{-}last}$ is the area under the curve from time zero to the last measurable concentration.

**Assay Procedures.** *Total and Intact IgG Assay.* As defined in Figure 1B, the Total IgG assay measured MEDI3726 and all catabolites that contain at least one heavy chain. The Intact IgG assay measures all forms of MEDI3726 and its catabolites that contain at least one heavy chain associated with one light chain. The assays relied on capture using protein G, thus capturing all forms regardless of the presence of the light chain or warhead.

Human plasma sample (40 μL) and 1× TBST with 1% (w/v) BSA buffer (100 μL) were mixed thoroughly before washed protein G magnetic beads (80 μL) were added for capture. After 2 h at room temperature with constant shaking, the beads were thoroughly washed with 1× TBS-based buffer. After washing with Kingfisher, a 40% (v/v) acetonitrile (ACN) solution (100 μL) was added to the beads in elution plate 1, thus eluting the light chain from the heavy chain attached to the beads. The heavy chains still being captured on the beads were then transferred to plate 2 with a Thermo Kingfisher and mixed with 50 mM ammonium bicarbonate (150 μL). Ammonium bicarbonate solution (50 mM, 150 μL) was added to elution plate 1. After elution of the LC, an internal standard solution was added to both plates. After shaking, Rapigest and DTT were added to both elution plates, followed by 1 h shaking and incubation at 60 °C. After reduction, alkylation was performed by adding IAA to both plates and incubating for 30 min, protected from light. Digestion was performed after alkylation by adding trypsin solution and incubating for 1.5 h at 37 °C with constant shaking. Hydrochloric acid (HCl, 2 N, 10 μL) was then added to the solution to quench the digestion. The contents from elution plates were passed through a filtration plate to the injection plates, respectively.

The Intact IgG assay monitored MEDI3726 and catabolites with at least one light chain and a heavy chain. From the eluate of plate 1, the light chain peptide ASQD (Table 1) was monitored. The separation was performed on a Waters UPLC BEH C18 column, with 0.1% formic acid in water as the aqueous mobile phase (MPA) and 0.1% formic acid and 0.2% DMSO in acetonitrile as the organic mobile phase (MPB). The gradient separation went from 10 to 30% MPB in 2.5 min, at 0.4 mL/min and 50 °C column temperature.

MEDI3726 and its catabolites with a heavy chain were monitored by the method denoted as the Total IgG assay. In the eluate from plate 2, the heavy chain peptide GLEW (Table 1) was monitored. The separation was performed on the aforementioned column with the same column temperature, mobile phases, and flow rate, with a separation gradient running from 10 to 20% MPB in 0.5 min and 20−24% MPB in 3 min.

*Total and Active ADC Assay.* The assays relied on capture using anti-PBD antibody, thus capturing all forms containing the warhead. The Total ADC assay measured MEDI3726 and all forms of its catabolites that contain at least one heavy chain with one warhead. The Active ADC assay measured MEDI3726 and all forms of its catabolites that contain at least one heavy chain with one warhead and one light chain.

Human plasma sample (50 μL) and TBST buffer with 1% BSA (100 μL) were mixed thoroughly before the addition of washed streptavidin M280 magnetic beads for the capture with anti-PBD antibody (50 μL). After capture overnight at 2−8 °C with constant shaking, the beads were thoroughly washed with a TBS-based wash buffer. After washing with Kingfisher, the beads were then transferred to the elution plate with a digestion buffer consisting of 10:20:70 methanol/1.0 M ammonium bicarbonate/water (v/v/v), RapiGest solution and DTT, followed by a 1 h shaking and incubation at 60 °C. After reduction, alkylation was performed by adding IAA to the elution plate and incubating for 30 min, protected from light. Digestion was performed after alkylation by adding trypsin solution and incubating for 1.5−2.0 h at 37 °C with constant shaking. After digestion, an internal standard solution was added. Additional ACN and HCl (2 N, 10 μL) was then added to the solution to quench digestion. The contents from elution plates were passed through a filtration plate into the injection plates.

Two peptides were monitored in this assay for the measurement of Total and Active ADC. For Total ADC, a heavy chain peptide (TSGY) was monitored; for Active ADC, a light chain peptide (ASQD) was monitored (Table 1). The separation was performed on a Waters UPLC BEH C18 column, with 0.1% formic acid in water as MPA, 0.1% formic acid in acetonitrile as MPB, and an additional mobile phase C (MPC) with 9% DMSO in 0.1% formic acid in ACN. The gradient separation went from 5 to 27% MPB in 1.5 min, 27% MPB held for 1.5 min, followed by 27−45% MPB in 2.5 min, at 0.2 mL/min and 50 °C column temperature. A separate pump with stainless steel tubing was used to deliver MPC at 0.1 mL/min during the elution period of the peptides.

*Total Conjugated ADC Assay.* The Total Conjugated ADC assay measured all the warhead conjugated to the heavy chain among MEDI3726 and all forms of its catabolites. MabSelect bead slurry (400 μL) was used in this assay to maximize the capturing capacity for all heavy chains that may have warhead conjugated. After the addition of 1% BSA in PBS (100 μL) to each well, 25 μL of human plasma was added to the MabSelect bead slurry that was preloaded to a filtration plate. The capture process lasted for 1 h with constant shaking at 2−8 °C. After capture the excessive liquid was filtered through. The plate was further washed multiple times with 20 mM ammonium acetate solution (200 μL each time). After washing, activated papain solution (2 mg/mL, 200 μL) was added to each well. The plate was sealed and incubated for 1 h at 25 °C. After the digestion with papain, the supernatant was filtered to the collection plate. An additional elution solution (70% ACN in water, 300 μL) was added to each well and also filtered to the collection plate. The SG3199-d10 IS solution (50 μL, 0.5 ng/mL) was added to all samples. After vortexing, the mixture in the collection plate was then dried under nitrogen gas. The residue was reconstituted with 30% ACN in water (25 μL) then protein-precipitated with methanol (100 μL). The plate was then vortexed and centrifuged. The supernatant (100 μL) was then transferred to the injection plate. HCl (0.2 N, 100 μL) and ammonium hydroxide (10%, 15 μL) were consecutively added to each sample. The plate was centrifuged before injection.

The cleaved warhead SG3199 was monitored in this assay for Total Conjugated ADC (Table 1). The separation was performed on a Kinetex Phenyl-Hexyl column with 0.1% formic acid, 20% ACN in water as MPA, 1% formic acid in methanol as MPB. The gradient for separation increased from 50 to 80% MPB in 0.8 min, at 0.4 mL/min, and 50 °C column temperature.

*Free Warhead Assay.* The Free Warhead assay quantified the free, unconjugated SG3199. Human plasma sample (50


https://dx.doi.org/10.1021/acs.analchem.0c01187
Anal. Chem. 2020, 92, 11135−11144

μL) was precipitated with methanol (70 μL). A volume of 150 μL of ACN based internal standard solution was added to the mixture. The plate was vortexed well followed by a 15 min centrifugation. The supernatant (100 μL) was transferred to the injection plate and mixed with 100 μL of water. The plate was then vortexed and centrifuged before injection.

The warhead SG3199 was monitored in this assay (Table 1). The separation was performed on a Kinetex Phenyl-Hexyl column with 0.1% formic acid, 20% ACN in water as MPA, 1% formic acid in methanol as MPB. The gradient for separation increased from 50 to 80% MPB in 0.8 min, at 0.4 mL/min, and 50 °C column temperature.

## RESULTS AND DISCUSSION

The aforementioned assays were successfully validated in human plasma (Table 1) and utilized during the first-in-human study of MEDI3726 (NCT02991911).[40,41]

**Possible Catabolites of MEDI3726 ADC.** For therapeutic proteins, the major clearance route is considered to be through the catabolic degradation from protease cleavage, in circulation and/or in tissues.[42,43] Besides the nonspecific protease cleavage, therapeutic proteins bound to the specific receptors on target cells can be cleared by target-mediated disposition.[42,43] Other factors that can contribute to the clearance of the biotherapeutics include antidrug antibodies as well as renal filtration. The latter is specifically applicable to low molecular weight biotherapeutics.[43] Despite the vast variety of potential catabolites that may be generated during the process, the regulatory guidance on the measurement of catabolites for biotherapeutics remains fairly limited. However, due to the emergence of many varied and novel biotherapeutic modalities, the necessity for more detailed characterization and quantification of various biotherapeutic catabolites should be re-evaluated. Since new modalities of therapeutic proteins may carry unique modifications, catabolite monitoring should be carefully evaluated for each molecule. In the specific case of MEDI3726, the catabolites that may impact its therapeutic index are the result of two unique modifications: the modified disulfide bonds and the conjugated payload. Since the interchain disulfide bonds were modified, there exists a potential for in vivo dissociation of both the light chain from the heavy chain as well as the two heavy chains from each other. Therefore, multiple forms of the free light chain and free heavy chain versions of MEDI3726 may be generated in vivo. Additionally, it is also possible that the PBD warhead would gradually deconjugate from the MEDI3726 heavy chain. Considering the combinatorial nature of the aforementioned possibilities, the potential MEDI3726 catabolites are described in Figure 1B. It has been previously reported that J591 scFv and Fab may still bind PSMA and internalize into cancer cells.[17,44] Therefore, among the metabolites of MEDI3726, the ones comprised of a heavy chain and a light chain could still possess the ability to bind PSMA and be internalized to deliver the warhead. However, the internalization rate and extent of the half antibody may differ from the complete MEDI3726.[45] Thus, we believe that the minimally pharmacologically active catabolite of MEDI3726 is the combination of the light chain, heavy chain, and the warhead.

**PK Characterization of MEDI3726 Catabolism.** MEDI3726 internalizes into target tumor cells through endocytosis and is degraded in lysosomes to release the conjugated PBD.[36] For an ADC, the controlled release of the toxin within the target tumor cell is critical to maximizing its therapeutic index. MEDI3726 catabolite species that contain both the heavy and light chains still maintain the IgG fold and are able to bind PSMA and, depending on whether or not they still have the warhead, may be able to exert tumor-killing activity. However, some inactive species such as the ones that contain merely the heavy chain with the warhead may pose a toxicity risk without contributing to efficacy. Nonetheless, current methodology employing surrogate analyte approaches cannot individually measure all of these catabolites.

The Active ADC assay measures the MEDI3726 species that contain at least one light chain associated with a heavy chain and one warhead attached to the heavy chain. These species maintain the ability to bind to the target receptor and deliver the small molecule drug. To better assess the concentration of all the conjugated warheads, either the Total ADC assay or a Total Conjugated ADC assay can be employed. Both assays monitor all the species of MEDI3726 and associated catabolites that still carry at least one warhead. The difference between these two assays resides in whether the conjugation of the warhead to the heavy chain is determined from the capture step vs the detection step. In the case of the Total ADC assay, the capture step is against the warhead with the detection of the heavy chain characteristic peptides. In the case of the Total Conjugated ADC assay, the capture is against the Fc and the detection is via the papain-released conjugated PBD warhead. Since the presence of conjugated warhead is determined differently in the two assays, it leads to a quantitative difference in the number of molar equivalents associated with some of the species quantified. Only one PBD molecule conjugated to the heavy chain is required for capture using the Total ADC assay. This accounts for the quantitative difference in results from the two assays for certain species, such as species that contain two heavy chains with only one warhead deconjugated from one of the heavy chains. The Intact IgG assay monitored MEDI3726 and associated catabolites that are able to bind to the target receptor. The Total IgG assay measures all species of MEDI3726 and associated catabolites that possess at least one heavy chain.

**Development and Optimization for Challenging Total and Intact IgG Assay.** Among the four methods described above, the most challenging assay to develop was the Total and Intact IgG assay. Since the target was to capture all species of MEDI3726 and associated catabolites in vivo, anti-IDs which usually bind to a specific region on the CDR or warhead and therefore can offer appropriate selectivity in the human matrix could not be used. Instead, a generic capture against the human IgG Fc region had to be employed. Since the capture was nonselective, it was critical that the detection peptides were highly selective. Careful optimization of the various parameters of the methods during development was required. This was achieved through the combination of careful sample cleanup, refined chromatography, and most importantly the selection of the unique MRM (multiple reaction monitoring) transitions. MEDI3726 light chain can be readily dissociated from the heavy chain with gentle elution conditions. This was exploited to enhance the selectivity of the Intact IgG assay. The elution step was optimized such that the light chain was eluted from the heavy chain while still on beads, enabling the desired sensitivity and selectivity for the Intact IgG assay. For the Total IgG assay, a thorough evaluation of the possible MRM transitions was necessary to achieve the selectivity requirement (Figure 3).


https://dx.doi.org/10.1021/acs.analchem.0c01187
Anal. Chem. 2020, 92, 11135−11144

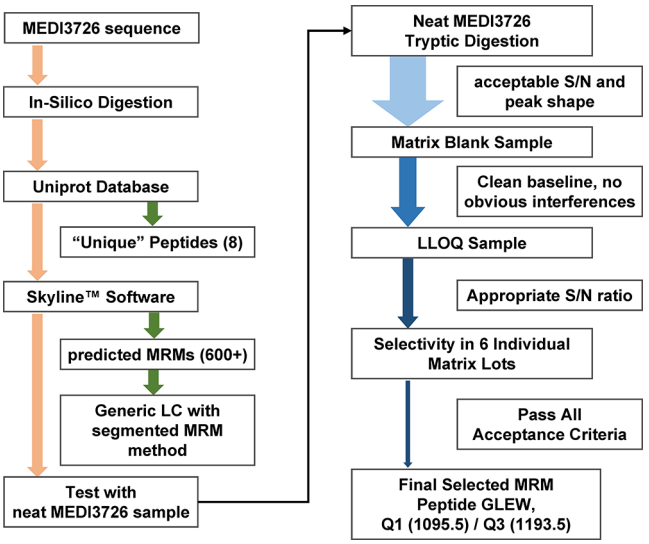


**Figure 3.** Development of the Total IgG assay. On the left is the in-silico preparation to generate the MRM transitions for evaluation. On the right is the MRM transition evaluation procedure.

To select the appropriate MRM transition for the Total IgG assay, MEDI3726 sequence was first subjected to the in-silico digestion and searched against the Uniprot Database (www.uniprot.org). The search results returned eight peptides that are unique in human plasma, see Supporting Information Table S1. These proteotypic "unique" peptides have a higher probability to contain MRMs that can be highly selective at the desired sensitivity. The Skyline software was used to generate 600+ possible MRM transitions[46] from these eight proteotypic peptides, including different charge states of the precursor ions and y&b fragment ions. Generic LC method was employed with the segmented predicted MRMs (about 20 MRMs per method) for the initial selection of the MRM transitions.

The first MRM evaluation utilized trypsin-digested neat MEDI3726 material. Only the MRMs with appropriate S/N and acceptable peak shape from this initial evaluation were used for the second round of evaluation. Matrix blank samples containing no MEDI3726 were digested and analyzed with generic LC methods. The ideal MRM candidate should have clean baseline with no obvious interference peaks at the selected mass transitions and expected retention times. After the second round of evaluation, the MRMs from the GLEW and TSGY peptides were selected for further evaluation at the LLOQ (lower limit of quantification) samples. The MRM transitions that had appropriate S/N ratio at the LLOQ level were further tested with selectivity blank, double blank and fortified at the LLOQ level prepared in plasma samples from six different matrix lots. GLEW peptide showed more selectivity than TSGY using the generic Protein G capture procedure and was selected for Total IgG assay. The final selection had to pass all the prespecified criteria for the Total IgG assay. On the other hand, TSGY peptide was successfully used for Total ADC assay using a more selective capture protocol (i.e., anti-PBD antibody). Similar approach has been applied to select a unique peptide from the light chain and the appropriate MRM transition for Intact IgG and Active ADC assays.

**Clinical PK data for MEDI3726.** Patients participating in the clinical study (NCT02991911) were dosed every 3 weeks (q3w) with escalating doses of MEDI3726.[41] The plasma samples were analyzed using the above-described methods. Representative data (from patients dosed with 0.25 mg/kg q3w MEDI3726) for the assays measuring MEDI3726 and its protein-containing catabolites are presented in Figure 4A. Bioanalytical considerations of assay variability, as assessed by accuracy and precision, apply to interpretation of these data when comparing results from the different assays. Generally, for the LBA-LC-MS/MS assays, the assay precision and accuracy were ≤20% across the dynamic range, with ≤25% at

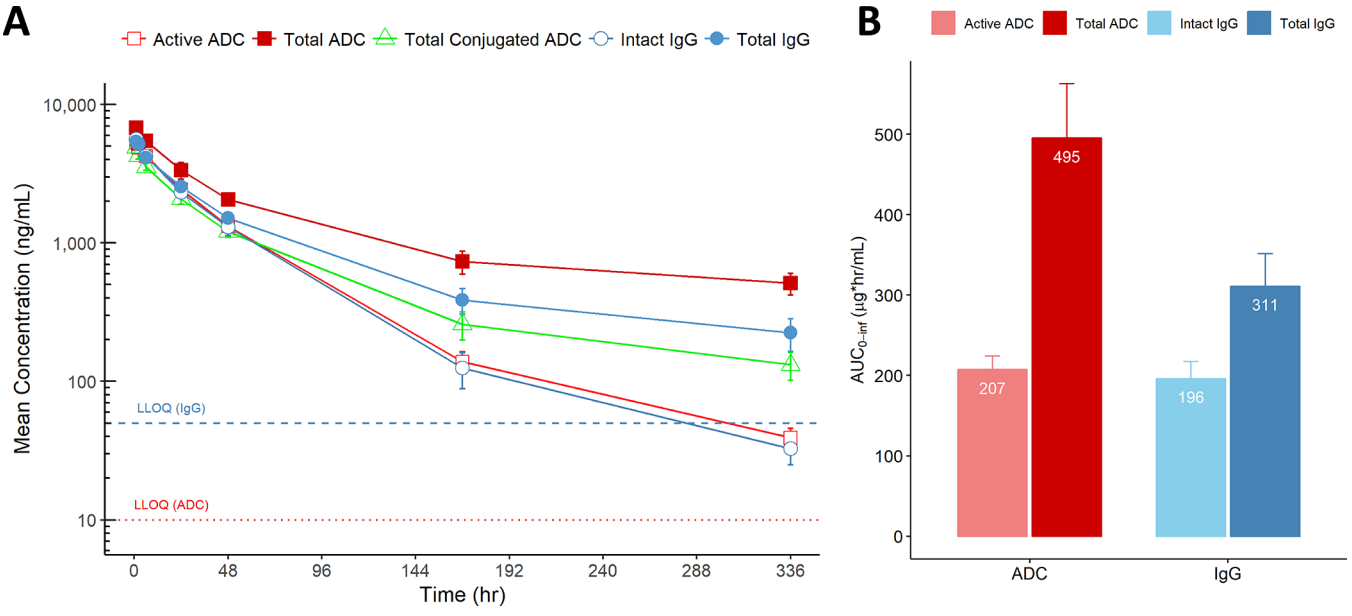


**Figure 4.** MEDI3726 and catabolites concentration−time profiles after the first dose of MEDI3726 at 0.25 mg/kg. $N = 6$, except for time point 336, where $N = 5$. Error bars represent the standard error of the mean. Below LLOQ values were set to 1/2 LLOQ for the calculation. (A) Mean concentration−time profiles of MEDI3726 and its catabolites. (B) Mean $AUC_{0\text{-inf}}$ of the Active and Total ADC and Intact and Total IgG assay. Mean $AUC_{0\text{-inf}}$ for Total Conjugated ADC was 225 $\mu$g h/mL (std. error = 22).



https://dx.doi.org/10.1021/acs.analchem.0c01187
Anal. Chem. 2020, 92, 11135−11144

LLOQ. However, the assay procedure for complex immunocapturing-LC-MS/MS methods (such as Total IgG and Intact IgG, or Total ADC and Active ADC assays) shared the same immunocapture enrichment step. In subsequent steps of the experimental procedure, the two detection surrogate analytes were processed separately. In assays that shared part of the procedure, the random difference between the assays may be smaller. In which case, it could be argued that the difference to be considered relevant once they differ by a smaller percentage. For instance, acceptance criteria for chromatographic assays (15/20) can be applicable. In order to better understand in vivo catabolism of MEDI3726, it is useful to consider changes in the composition of various MEDI3726 species within the same patient as manifested by the readout of the assays employed (Figure 4B). Shortly after administration of MEDI3726, most of the species detected by surrogate analytes employed would be well represented by the parent drug, MEDI3726. At later time points, MEDI3726 will be catabolized and additional species would appear. It may be helpful to evaluate the changes for catabolites for each individual patient as the changes related to metabolism of the target compound may vary depending on the patient.

The Active ADC assay most accurately represents the concentrations of the MEDI3726 alone. Therefore, it should be used as the foundation for comparisons between the assays. For example, comparing the Active ADC and Total ADC assays can provide information on the dissociation of light chain from heavy chain. The comparison of Intact IgG and Total IgG assays can provide similar information. On the other hand, the comparison of the Intact IgG and Active ADC assays can help assess the deconjugation of warhead.

The catabolites of MEDI3726 that present the most concern with respect to the therapeutic index were the free warhead as well as warhead conjugated only to heavy chain (as it cannot recognize target in the absence of light chain, data not shown). The comparison of Active ADC and Intact IgG profiles indicated minimal deconjugation of the warhead in vivo (except for patient A, see the Supporting Information, Figure S7). However, since the LLOQ for these two assays are different (Table 1), the observed divergence in profiles of the two measurements for patient A could be attributed to differences in the assay sensitivity. Moreover, the mean AUC ratio between Intact IgG and Active ADC was around 1, indicating no difference between these two analyses (Figure 4B). This result, together with the data from the free warhead assay being largely below LLOQ (LLOQ = 20 pg/mL, data not shown), demonstrated that there was negligible deconjugation of the warhead observed in vivo up until at least 14 days.

On the other hand, comparison of the Active ADC assay vs the Total ADC assay in Figure 4A indicated separation over time. Similar observation can be made comparing the Intact IgG assay vs the Total IgG assay. The separation of the profiles quantified by these sets of complementary assays was >50%, from the 168-h time point and beyond (Figure 4A). From the PK profiles in Figure 4A, the majority of conjugated ADC at the end of the dosing interval is likely to be in the form of warhead-conjugated heavy chain, which is unable to bind to the target. In terms of the total PK exposure as indicated by AUC, both total ADC and total IgG were 2.3- and 1.6-fold higher, respectively, when compared to Active ADC and Intact IgG assay (Figure 4B). The distinction between the readouts of these assays resides in the measurement of the light chain signature peptide versus the heavy chain signature peptide. The combination of these data suggested that as MEDI3726 was present in circulation for a sufficient time, the difference in concentrations of the light chain associated with the heavy chain conjugated with the warhead vs heavy chain alone becomes more significant with time. This was evident from the $AUC_{0\text{-inf}}$ (area under curve) calculated from the different assays (Figure 4B and Supporting Information, Figure S8). Similar results were observed for the individual patients (Supporting Information, Figure S7), suggesting that this may be a common catabolic pathway for MEDI3726. The catabolic profile of MEDI3726 is the combination of several processes: generation of various species deriving from MEDI3726 as well as their elimination from circulation. The determination of the kinetics of the various catabolites will require more detailed characterization.

## CONCLUSION

Recent advances in protein engineering have led to the emergence of novel biotherapeutic modalities with innovative structural design and distinct functionalities while presenting additional considerations with respect to their efficacy, safety, immunogenicity, as well as pharmacokinetic properties. The new modalities present novel challenges for characterization of PK and metabolism of these molecules. This deeper characterization should not only improve the understanding of the factors impacting the therapeutic index as well as the mechanism of action for the unique functions of new modalities, but also will shed light on the future improvement of drug design. Herein, we presented an example of detailed bioanalytical methods required to assess PK and catabolism of the unique ADC, MEDI3726. The bioanalysis strategy was defined by the considerations of structure, the evaluation of anticipated catabolism, and the necessity of rigorous monitoring of potentially toxic catabolites and balanced with the limitations of current advanced bioanalytical techniques. A detailed characterization to such an extent may not be common for a well-understood traditional mAb but is recommended for novel modalities, especially for the first-in-human studies. In particular, for stochastically cysteine-conjugated ADCs, particularly with high DAR, the probability of disruption of interchain disulfide bonds is high. Nonetheless, while multiple ADCs with engineered cysteines have been tested in clinical trials, there are no approved ADCs with engineered cysteine-conjugates to date. Among the eight ADC drugs that have been approved by the FDA so far, five contained cysteine conjugation that replaces the interchain disulfide bonds with various toxins conjugated at different DAR. Such a conjugation strategy will result in a complex catabolite profile for the ADC in question and may affect its therapeutic index. Further characterization of in vivo catabolism of complex biotherapeutics will require development of novel bioanalytical methods employing high-resolution accurate mass spectrometry (HRMS) using intact protein analyses as well as proteomic-type experiments. Such approaches would be able to provide more detailed information about individual species and potentially uncover additional modifications not observed with targeted approaches.

## ASSOCIATED CONTENT

### Supporting Information

The Supporting Information is available free of charge at https://pubs.acs.org/doi/10.1021/acs.analchem.0c01187.



https://dx.doi.org/10.1021/acs.analchem.0c01187
Anal. Chem. 2020, 92, 11135−11144

General reagents, representative chromatograms, individual concentration−time profiles, area under the curve for hybrid LBA-LC−MS/MS assays, and sequences of unique proteotypic tryptic peptides (PDF)

## AUTHOR INFORMATION


### Corresponding Author

**Anton I. Rosenbaum** − *Integrated Bioanalysis, Clinical Pharmacology, and Quantitative Pharmacology, Clinical Pharmacology & Safety Sciences, R&D, AstraZeneca, South San Francisco, California 94080, United States;* orcid.org/0000-0003-1939-951X; Phone: +1-650-379-3099; Email: anton.rosenbaum@astrazeneca.com

### Authors

**Yue Huang** − *Integrated Bioanalysis, Clinical Pharmacology, and Quantitative Pharmacology, Clinical Pharmacology & Safety Sciences, R&D, AstraZeneca, South San Francisco, California 94080, United States;* orcid.org/0000-0003-2788-0856

**Christopher J. Del Nagro** − *Integrated Bioanalysis and Clinical Pharmacology, AstraZeneca, South San Francisco, California 94080, United States*

**Kemal Balic** − *Clinical Pharmacology and Quantitative Pharmacology, Clinical Pharmacology & Safety Sciences, R&D, AstraZeneca, South San Francisco, California 94080, United States*

**William R. Mylott Jr.** − *PPD Laboratories, Richmond, Virginia 23230, United States*

**Omnia A. Ismaiel** − *PPD Laboratories, Richmond, Virginia 23230, United States; Department of Pharmaceutical Analytical Chemistry, Faculty of Pharmacy, Zagazig University, Zagazig, Sharkia 44519, Egypt*

**Eric Ma** − *PPD Laboratories, Richmond, Virginia 23230, United States*

**Morse Faria** − *PPD Laboratories, Richmond, Virginia 23230, United States*

**Aaron M. Wheeler** − *PPD Laboratories, Richmond, Virginia 23230, United States*

**Moucun Yuan** − *PPD Laboratories, Richmond, Virginia 23230, United States*

**Michael P. Waldron** − *PPD Laboratories, Richmond, Virginia 23230, United States*

**Marlking G. Peay** − *PPD Laboratories, Richmond, Virginia 23230, United States*

**Diego F. Cortes** − *PPD Laboratories, Richmond, Virginia 23230, United States*

**Lorin Roskos** − *Clinical Pharmacology and Quantitative Pharmacology, Clinical Pharmacology & Safety Sciences, R&D, AstraZeneca, South San Francisco, California 94080, United States*

**Meina Liang** − *Integrated Bioanalysis, Clinical Pharmacology, and Quantitative Pharmacology, Clinical Pharmacology & Safety Sciences, R&D, AstraZeneca, South San Francisco, California 94080, United States*

Complete contact information is available at: https://pubs.acs.org/10.1021/acs.analchem.0c01187


### Author Contributions

The manuscript was written through contributions of all authors. All authors have given approval to the final version of the manuscript.

### Notes

The authors declare the following competing financial interest(s): PPD-affiliated coauthors have declared no competing financial interests. AstraZeneca provided funding to PPD for the conduct of this study. Yue Huang, Meina Liang, and Anton Rosenbaum are employees of AstraZeneca and have stock ownership and/or stock interests or options in the company. Kemal Balic, Christopher Del Nagro and Lorin Roskos were employees of AstraZeneca at the time this research was conducted, with stock ownership and/or stock interests or options in the company.

## ACKNOWLEDGMENTS

We would like to thank Brandon Lam for his contributions to the project and Gary Prohaska and Daniel Nagy for the graphic design.

## REFERENCES


(1) Siegel, R. L.; Miller, K. D.; Jemal, A. *Ca-Cancer J. Clin.* **2019**, *69* (1), 7−34.

(2) Wang, X.; Ma, D.; Olson, W. C.; Heston, W. D. *Mol. Cancer Ther.* **2011**, *10* (9), 1728−39.

(3) Ma, D.; Hopf, C. E.; Malewicz, A. D.; Donovan, G. P.; Senter, P. D.; Goeckeler, W. F.; Maddon, P. J.; Olson, W. C. *Clin. Cancer Res.* **2006**, *12* (8), 2591−6.

(4) Wolf, P.; Gierschner, D.; Buhler, P.; Wetterauer, U.; Elsasser-Beile, U. *Cancer Immunol. Immunother.* **2006**, *55* (11), 1367−73.

(5) Israeli, R. S.; Powell, C. T.; Corr, J. G.; Fair, W. R.; Heston, W. D. *Cancer Res.* **1994**, *54* (7), 1807−1811.

(6) Israeli, R. S.; Miller, W. H., Jr.; Su, S. L.; Powell, C. T.; Fair, W. R.; Samadi, D. S.; Huryk, R. F.; DeBlasio, A.; Edwards, E. T.; Wise, G. J. *Cancer Res.* **1994**, *54* (24), 6306−6310.

(7) Trover, J. K.; Beckett, M. L.; Wright, G. L. *Int. J. Cancer* **1995**, *62* (5), 552−558.

(8) Murphy, G. P.; Elgamal, A. A.; Su, S. L.; Bostwick, D. G.; Holmes, E. H. *Cancer* **1998**, *83* (11), 2259−69.

(9) Sweat, S. D.; Pacelli, A.; Murphy, G. P.; Bostwick, D. G. *Urology* **1998**, *52* (4), 637−40.

(10) Gregorakis, A. K.; Holmes, E. H.; Murphy, G. P. *Semin. Urol. Oncol.* **1998**, *16* (1), 2−12.

(11) Brown, L. G.; Wegner, S. K.; Wang, H.; Buhler, K. R.; Arfman, E. W.; Lange, P. H.; Vessella, R. L. *Prostate Cancer Prostatic Dis.* **1998**, *1* (4), 208−215.

(12) Gong, M. C.; Chang, S. S.; Sadelain, M.; Bander, N. H.; Heston, W. D. *Cancer Metastasis Rev.* **1999**, *18* (4), 483−90.

(13) Bander, N. H.; Nanus, D. M.; Milowsky, M. I.; Kostakoglu, L.; Vallabahajosula, S.; Goldsmith, S. J. *Semin. Oncol.* **2003**, *30* (5), 667−76.

(14) Bander, N. H.; Trabulsi, E. J.; Kostakoglu, L.; Yao, D.; Vallabhajosula, S.; Smith-Jones, P.; Joyce, M. A.; Milowsky, M.; Nanus, D. M.; Goldsmith, S. J. *J. Urol.* **2003**, *170* (5), 1717−21.

(15) Li, Y.; Tian, Z.; Rizvi, S. M.; Bander, N. H.; Allen, B. J. *Prostate Cancer Prostatic Dis.* **2002**, *5* (1), 36−46.

(16) Holmes, E. H. *Expert Opin. Invest. Drugs* **2001**, *10* (3), 511−9.

(17) Liu, H.; Rajasekaran, A. K.; Moy, P.; Xia, Y.; Kim, S.; Navarro, V.; Rahmati, R.; Bander, N. H. *Cancer Res.* **1998**, *58* (18), 4055−4060.

(18) Petrylak, D. P.; Kantoff, P.; Vogelzang, N. J.; Mega, A.; Fleming, M. T.; Stephenson, J. J., Jr.; Frank, R.; Shore, N. D.; Dreicer, R.; McClay, E. F.; Berry, W. R.; Agarwal, M.; DiPippo, V. A.; Rotshteyn, Y.; Stambler, N.; Olson, W. C.; Morris, S. A.; Israel, R. J. *Prostate* **2019**, *79* (6), 604−613.

(19) Lutje, S.; Gerrits, D.; Molkenboer-Kuenen, J. D.; Herrmann, K.; Fracasso, G.; Colombatti, M.; Boerman, O. C.; Heskamp, S. *J. Nucl. Med.* **2018**, *59* (3), 494−501.

(20) DiPippo, V. A.; Nguyen, H. M.; Brown, L. G.; Olson, W. C.; Vessella, R. L.; Corey, E. *Prostate* **2016**, *76* (3), 325−34.

(21) Kumar, A.; Mastren, T.; Wang, B.; Hsieh, J. T.; Hao, G.; Sun, X. *Bioconjugate Chem.* **2016**, *27* (7), 1681−9.
(22) Milowsky, M. I.; Galsky, M. D.; Morris, M. J.; Crona, D. J.; George, D. J.; Dreicer, R.; Tse, K.; Petruck, J.; Webb, I. J.; Bander, N. H.; Nanus, D. M.; Scher, H. I. *Urol. Oncol.* **2016**, *34* (12), 530.e15 e15−530 e21..
(23) Sassoon, I.; Blanc, V. *Methods Mol. Biol.* **2013**, *1045*, 1−27.
(24) Anderl, J.; Faulstich, H.; Hechler, T.; Kulke, M. *Methods Mol. Biol.* **2013**, *1045*, 51−70.
(25) Ricart, A. D. *Clin. Cancer Res.* **2011**, *17* (20), 6417−27.
(26) Gualberto, A. *Expert Opin. Invest. Drugs* **2012**, *21* (2), 205−16.
(27) Challita-Eid, P. M.; Satpayev, D.; Yang, P.; An, Z.; Morrison, K.; Shostak, Y.; Raitano, A.; Nadell, R.; Liu, W.; Lortie, D. R.; Capo, L.; Verlinsky, A.; Leavitt, M.; Malik, F.; Avina, H.; Guevara, C. I.; Dinh, N.; Karki, S.; Anand, B. S.; Pereira, D. S.; Joseph, I. B.; Donate, F.; Morrison, K.; Stover, D. R. *Cancer Res.* **2016**, *76* (10), 3003−13.
(28) Niculescu-Duvaz, I. *Curr. Opin. Mol. Ther.* **2010**, *12* (3), 350−360.
(29) Deeks, E. D. *Drugs* **2019**, *79*, 325.
(30) Tamura, K.; Tsurutani, J.; Takahashi, S.; Iwata, H.; Krop, I. E.; Redfern, C.; Sagara, Y.; Doi, T.; Park, H.; Murthy, R. K.; Redman, R. A.; Jikoh, T.; Lee, C.; Sugihara, M.; Shahidi, J.; Yver, A.; Modi, S. *Lancet Oncol.* **2019**, *20* (6), 816−826.
(31) Shitara, K.; Iwata, H.; Takahashi, S.; Tamura, K.; Park, H.; Modi, S.; Tsurutani, J.; Kadowaki, S.; Yamaguchi, K.; Iwasa, S.; Saito, K.; Fujisaki, Y.; Sugihara, M.; Shahidi, J.; Doi, T. *Lancet Oncol.* **2019**, *20* (6), 827−836.
(32) Tolcher, A. W. *Am. Soc. Clin. Oncol. Educ. Book* **2020**, *40*, 127−134.
(33) Bardia, A.; Mayer, I. A.; Vahdat, L. T.; Tolaney, S. M.; Isakoff, S. J.; Diamond, J. R.; O'Shaughnessy, J.; Moroose, R. L.; Santin, A. D.; Abramson, V. G.; Shah, N. C.; Rugo, H. S.; Goldenberg, D. M.; Sweidan, A. M.; Iannone, R.; Washkowitz, S.; Sharkey, R. M.; Wegener, W. A.; Kalinsky, K. *N. Engl. J. Med.* **2019**, *380* (8), 741−751.
(34) Flynn, M. J.; Zammarchi, F.; Tyrer, P. C.; Akarca, A. U.; Janghra, N.; Britten, C. E.; Havenith, C. E.; Levy, J. N.; Tiberghien, A.; Masterson, L. A.; Barry, C.; D'Hooge, F.; Marafioti, T.; Parren, P. W.; Williams, D. G.; Howard, P. W.; van Berkel, P. H.; Hartley, J. A. *Mol. Cancer Ther.* **2016**, *15* (11), 2709−2721.
(35) Zammarchi, F.; Corbett, S.; Adams, L.; Tyrer, P. C.; Kiakos, K.; Janghra, N.; Marafioti, T.; Britten, C. E.; Havenith, C. E. G.; Chivers, S.; D'Hooge, F.; Williams, D. G.; Tiberghien, A.; Howard, P. W.; Hartley, J. A.; van Berkel, P. H. *Blood* **2018**, *131* (10), 1094−1105.
(36) Cho, S.; Zammarchi, F.; Williams, D. G.; Havenith, C. E. G.; Monks, N. R.; Tyrer, P.; D'Hooge, F.; Fleming, R.; Vashisht, K.; Dimasi, N.; Bertelli, F.; Corbett, S.; Adams, L.; Reinert, H. W.; Dissanayake, S.; Britten, C. E.; King, W.; Dacosta, K.; Tammali, R.; Schifferli, K.; Strout, P.; Korade, M., 3rd; Masson Hinrichs, M. J.; Chivers, S.; Corey, E.; Liu, H.; Kim, S.; Bander, N. H.; Howard, P. W.; Hartley, J. A.; Coats, S.; Tice, D. A.; Herbst, R.; van Berkel, P. H. *Mol. Cancer Ther.* **2018**, *17* (10), 2176−2186.
(37) Saber, H.; Simpson, N.; Ricks, T. K.; Leighton, J. K. *Regul. Toxicol. Pharmacol.* **2019**, *107*, 104429.
(38) Mou, S.; Huang, Y.; Rosenbaum, A. I. *Antibodies* **2018**, *7* (4), 41.
(39) Tiberghien, A. C.; Levy, J. N.; Masterson, L. A.; Patel, N. V.; Adams, L. R.; Corbett, S.; Williams, D. G.; Hartley, J. A.; Howard, P. W. *ACS Med. Chem. Lett.* **2016**, *7* (11), 983−987.
(40) De Bono, J. S.; Fleming, M. T.; Wang, J. S.-Z.; Cathomas, R.; Williams, M.; Bothos, J. G.; Balic, K.; Cho, S. H.; Martinez, P.; Petrylak, D. P. *J. Clin. Oncol.* **2020**, *38* (6_suppl), 99−99.
(41) *A Phase 1/1b Study of MEDI3726 in Adults Subjects With Metastatic Castration Resistant Prostate Cancer*, https://ClinicalTrials.gov/show/NCT02991911.
(42) Ezan, E.; Becher, F.; Fenaille, F. *Expert Opin. Drug Metab. Toxicol.* **2014**, *10* (8), 1079−91.
(43) Hamuro, L. L.; Kishnani, N. S. *Bioanalysis* **2012**, *4* (2), 189−95.
(44) Parker, S. A.; Diaz, I. L.; Anderson, K. A.; Batt, C. A. *Protein Expression Purif.* **2013**, *89* (2), 136−45.
(45) Goulet, D. R.; Atkins, W. M. *J. Pharm. Sci.* **2020**, *109* (1), 74−103.
(46) Pino, L. K.; Searle, B. C.; Bollinger, J. G.; Nunn, B; MacLean, B.; MacCoss, M. J. *Mass Spectrom. Rev.* **2020**, *39* (3), 229−244.


https://dx.doi.org/10.1021/acs.analchem.0c01187
*Anal. Chem.* 2020, 92, 11135−11144